 CMES, vol.102, no.5, pp.373-391, 2014

An Improved Isogeometric Boundary Element Method Approach in Two Dimensional Elastostatics

Vincenzo Mallardo[1] **and Eugenio Ruocco**[2]

Abstract: The NURBS based isogeometric analysis offers a novel integration between the CAD and the numerical structural analysis codes due to its superior capacity to describe accurately any complex geometry. Since it was proposed in 2005, the approach has attracted rapidly growing research interests and wide applications in the Finite Element context. Only recently, in 2012, it was successfully tested together with the Boundary Element Method. The combination of the isogeometric approach and the Boundary Element Method is efficient since both the NURBS geometrical representation and the Boundary Element Method deal with quantities entirely on the boundary of the problem. Actually, there are still some difficulties in imposing generic boundary conditions, mainly due to the fact that the NURBS basis functions are not interpolatory functions. In this work it is shown that the direct imposition of the inhomogeneous generic boundary conditions to the NURBS control points may lead to significant errors. Consequently an improved formulation is proposed that relates the boundary conditions to the governing unknown variables by developing a transformation strategy. Several elasticity problems evince that higher solution accuracy can be achieved by the present formulation.

Keywords: NURBS, Isogeometric analysis, Mixed boundary conditions, Transformation method, Boundary Element Method, IGABEM.

1 Introduction

From the structural point of view, design in engineering and architecture usually passes through two main steps: 1) the generation of the geometry, 2) the analysis of the structure. As a matter of fact these two steps do not progress as independent phases. The first step encompasses the definition of the main geometry of the

[1] University of Ferrara, Department of Architecture, via Quartieri 8, 44121 Ferrara (Italy). E-mail: mlv@unife.it, corresponding author.
[2] Second University of Naples, Department of Civil Engineering, Design, Building and Environment, via Roma, 29, Aversa, Caserta (Italy). E-mail: eugenio.ruocco@unina2.it

element under analysis (i.e. a building, a bridge, an airplane, a ship, etc.) along with all the architectural and technological details that are necessary to present it in its final configuration, i.e. the configuration that is the closest possible to what will appear when built. Such a design step should proceed simultaneously to the structural analysis in order to configure a final solution that correctly interfaces the structure with the geometry. Therefore a repetitive structural analysis is required both to adapt the structure to the continuous modifications in the architecture that are necessary to achieve the "best" design and to refine the model for accuracy improvements.

There are two main hurdles in combining the geometrical design with the structural design. First of all the "structural geometry" is different from the "architectural" geometry; the former only contains the skeleton, i.e. columns, beams, bearing plates and shells, etc., and it does not give prominence to structurally unnecessary features, i.e. components that do not have relevant bearing properties. Secondly, the tools used to design the geometry are different from the ones that are used to model and mesh the structure.

In the common engineering approach the geometry of the problem is modeled in the Computer Aided Design (CAD) context, whereas the mechanical behavior is obtained by reproducing a new model in a Computer Aided Engineering Software (CAE). As underlined by Hughes, Cottrell, and Bazilev (2005), the different geometric representation between the CAD system and the computational mechanics context is probably related to the fact that they had the origin in different time, i.e. CAD about twenty years later. The construction of the structural geometry (i.e. the mesh) is costly and time consuming. In fact the main drawback of the Finite Element Method (FEM) is the lack of an exact geometry representation for complex engineering shapes, usually defined by polynomial curves and conic sections. The accuracy of the approximation depends on the size of the used mesh and each refinement iteration requires interaction with the geometry. This may result in a very expensive process for complex geometries. Moreover, the geometric approximation inherent in the mesh can lead to accuracy problems. It is clear that any attempt to change the mesh generation and refinement with something more CAD-like is very welcome.

In CAD software the geometry is governed by the use of B-Spline and Non Uniform Rational B-Splines (NURBS, see Piegl and Tiller (1997)) curves, where control points, knot vectors and weights are the main ingredients. On the other hand in CAE the geometry is linked to the governing variables by the polynomial shape functions. Hughes, Cottrell, and Bazilev (2005) represents the first attempt to describe the Finite Element (FE) model as given by a CAD system, i.e. in terms of standard CAD representations like B-spline or NURBS. The geometry is exactly represented and preserved since the coarsest refinement level and mesh refinement turn out to be highly simplified by standard knot-insertion and/or degree-raising procedures, eliminating the need to communicate with the CAD system after the mesh construction. Being the solution space for the governing variables represented in terms of the same functions which represent the geometry justifies the tag of IsoGeometric Analysis (IGA).

In Cho, Choi, and Roh (2008) the NURBS were constructed by the data extracted from the CAD-generated IGES format file in the shell finite element framework.

A NURBS-based parametric mesh free method (NPMM) was also proposed three years later in Shaw and Roy (2008): the FE-based domain discretization is combined with the global smoothness polynomial reproducing shape functions constructed through NURBS. Shaw, Banerjee, and Roy (2008) extended the applicability of NPMM in order to preserve the bijection between the physical domain and the parametric domain that was not guaranteed everywhere in the previous paper. Such a method has been successfully applied to several linear and nonlinear solid mechanics problems. However, one of its problematic issue is a possible nonconformality in the numerical integration owing to the dual use of knots as particles (or nodes) whilst constructing the NURBS bases. A significant improvement of this concept was addressed in Sunilkumar and Roy (2010).

A NURBS-enhanced FEM, both in two dimensional (2D) and in three dimensional (3D) potential problems, was proposed in Sevilla, Fernández-Méndez, and Huerta (2008), Sevilla, Fernández-Méndez, and Huerta (2011), respectively. The idea is to describe the boundary of the computational domain (and not the entire domain) by the NURBS but to approximate the solution by standard piecewise polynomials in the physical space. The methodology is simpler and the main advantage is that standard FE interpolation and numerical integration can be used, preserving the computational efficiency of classical FE techniques.

The B-spline can also be used for different purposes. In Sageresan and Drathi (2008), for instance, the normalized quartic B-spline was used to average the stress tensor to avoid spurious crack path oscillations in a meshless approach to crack propagation in concrete.

The Boundary Element Method (BEM) has demonstrated to be a valid alternative to FEM in many areas of interest (see for instance Wrobel and Aliabadi (1996)), with special emphasis to infinite problems and crack analysis. The main advantage stands in the discretization, that is limited to the boundary but it needs to be extended to one or more internal areas if some nonlinearities occur (see for instance Mallardo (2009) in damage analysis). Coupling with the Fast Multipole Method has increased the performance of BEM and it has reduced the required CPU time (see for instance Mallardo and Aliabadi (2012) in acoustic). To combine the isogeometric approach with the BEM can be very efficient. One reason stems from the involvement of the boundary only in the CAD softwares. Another reason is related to the fact that computed quantities on boundaries are the most important ones in engineering applications, and this is where geometric errors are most harmful.

The very first attempt to couple BEM with the isogeometric analysis (IGABEM) is presented in Simpson, Bordas, Trevelyan, and Rabczuk (2012). The NURBS are adopted to represent both the geometry and the physical governing quantities in 2D elastostatics. Some numerical examples, i.e. the problem of a hole within an infinite plate, the L-shaped wedge and the open spanner, are shown to demonstrate the efficiency of the procedure. It must be underlined that the issue of the correct imposition of the BCs is not pursued as inhomogeneous Neumann conditions are always applied at straight lines. Implementation details (in Matlab) of the above contribution are given in Simpson, Bordas, Lian, and Trevelyan (2013).

The procedure is extended to 2D Helmholtz problems in Peake, Trevelyan, and Coates (2013). In the same paper the Authors proceed further by combining the partition of unity method in BEM with the isogeometric approach, giving rise to what they call eXtended Isogeometric BEM (XIBEM).

An interesting application of the Fast Multipole Method (FMM) to IGABEM is given in Takahashi and Matsumoto (2012) for Laplace equation in 2D. Some examples are shown to demonstrate that the proposed procedure possesses the same accuracy of the IGABEM but a better complexity (of order $O(n)$).

Both in BEM coupled with IGA and in FEM coupled with IGA, special attention must be paid to the imposition of the boundary conditions. The unknowns are parameters that have no physical meaning whereas the boundary conditions are to be applied in terms of either displacement or traction to boundary points. The issue is not raised if either the curve is interpolatory or constant boundary conditions are applied on the element. Inhomogeneous boundary conditions are usually directly imposed to the control points Hughes, Cottrell, and Bazilev (2005), Simpson, Bordas, Trevelyan, and Rabczuk (2012), i.e. the function describing the boundary conditions is evaluated at the spatial locations of the control points and then the resultant values are assigned to the corresponding control variables. In case that the boundary control points do not lay on the desired boundary such an approach implies a poor approximation of the boundary conditions which reflects on the accuracy of the solution.

In the FE context there are two main papers proposing strategies that overcome the problem. One procedure involving quasi-interpolant projectors is proposed in Costantini, Manni, Pelosi, and Sampoli (2010) in the context of generalized B-spline based isogeometric analysis; no numerical examples are given in elasticity. A different procedure is proposed in Wang and Xuan (2010) by employing a transformation method to relate the control variables to the collocated nodal values at the essential boundary. The task is carried out by previously partitioning the NURBS control points into boundary and interior groups. Several elasticity analyses evince that much higher solution accuracy and better convergence rates can be achieved by the proposed improved formulation.

In the present paper an improved IGABEM approach is proposed to correctly apply the boundary conditions to the boundary points. Such an enhancement has never been considered so far to the best knowledge of the Authors. A technique is implemented to correctly deal with any boundary condition, regardless of the position of the control points with respect to the boundary line and regardless of the type (displacement or traction) and value imposed on the boundary.

The paper is organized as follows. The next section presents the NURBS and some of their properties of special interest in computational mechanics. The third section is devoted to provide the main features of the conventional BEM and of the IGA-BEM approach. The fourth section is aimed at detailing the procedure proposed to correctly apply any boundary condition. The final section presents a numerical example to demonstrate the efficiency of the proposed procedure.

2 B-spline and NURBS

It is known that the most common methods of representing curves and surfaces in geometric modeling are implicit equations and parametric functions. In parametric form, each of the coordinates of a point on a 2D curve is represented separately as an explicit function of an independent parameter:

$$\mathbf{C}(\zeta) = (x_1(\zeta), x_2(\zeta)) \qquad a \leq \zeta \leq b \tag{1}$$

Although the interval $[a, b]$ is arbitrary it is here normalized to $[0, 1]$.

The definition of the NURBS passes through the definition of the B-spline (see chapters 2-4 of Piegl and Tiller (1997) for further details). In fact the NURBS are given by the following relation:

$$R_{i,p}(\zeta) = \frac{N_{i,p}(\zeta) w_i}{\sum_{j=1}^{n} N_{j,p}(\zeta) w_j} \tag{2}$$

where w_j are weights, $N_{i,p}(\zeta)$ is the i^{th} B-spline of degree p and n is the number of control points, i.e. some points (to be discussed further) that fulfill the same task of the mesh nodes in the conventional BEM.

In order to define the B-splines it is necessary to introduce the knot vector $U = (0,\cdots,\zeta_{i-1},\zeta_i,\zeta_{i+1},\cdots,1)$, i.e. a nondecreasing sequence of $n+p+1$ real numbers (normalised in $[0,1]$) where ζ_i are called knots. In the present contribution uniform knot vectors are considered, i.e. all interior knots are equally spaced. It must be underlined that the knot span, i.e. the half-open interval $[\zeta_i,\zeta_{i+1})$, can have zero length as the knots must not be necessarily distinct.

There is a number of ways to define the B-spline basis functions; the recurrence formula is here adopted as the most useful for computer implementation. The i^{th} B-spline of *0*-degree (order 1) can be hence defined as:

$$N_{i,0}(\zeta) \quad = \quad \begin{cases} 1 & \text{if } \zeta_i \leq \zeta < \zeta_{i+1} \\ \\ 0 & \text{otherwise} \end{cases} \tag{3}$$

The i^{th} B-spline of p-degree (order $p+1$) is defined as ($p>0$):

$$N_{i,p}(\zeta) \quad = \quad \frac{\zeta-\zeta_i}{\zeta_{i+p}-\zeta_i}N_{i,p-1}(\zeta)+\frac{\zeta_{i+p+1}-\zeta}{\zeta_{i+p+1}-\zeta_{i+1}}N_{i+1,p-1}(\zeta) \tag{4}$$

Eq. 3-Eq. 4 may yield the quotient $\frac{0}{0}$; by definition such a quotient is set to zero. The $N_{i,p}$ are piecewise polynomials defined on the entire boundary line, i.e. the line going from $\zeta=0$ to $\zeta=1$, but each is different from zero only in a part of it.

It is clear that $N_{i,0}$ is the well-known step function, zero everywhere except on the half open interval $\zeta\in[\zeta_i,\zeta_{i+1})$, and that the computation of the function $N_{i,p}$ requires the specification of the degree p and of the knot vector U. The above B-splines benefit from some properties that reveal to be very useful in the context under analysis:

- $N_{i,p}(\zeta)=0$ if ζ is outside the interval $[\zeta_i,\zeta_{i+p+1})$.
- Therefore, in any given knot span $[\zeta_j,\zeta_{j+1})$ at most $p+1$, i.e. $N_{j-p,p}\cdots N_{j,p}$, of the $N_{i,p}$ are non zero.
- For an arbitrary knot span $[\zeta_i,\zeta_{i+1})$, $\sum_{j=i-p}^{i}N_{j,p}(\zeta)=1$ for all $\zeta\in[\zeta_i,\zeta_{i+1})$.

The last property implies that each B-spline does not necessarily assume the unit value in one knot and zero elsewhere, as it occurs with the classical polynomial shape functions.

The derivative of B-spline is necessary to compute the stress in any internal point. Such derivatives are given by:

$$N'_{i,p}(\zeta)=\frac{p}{\zeta_{i+p}-\zeta_i}N_{i,p-1}(\zeta)-\frac{p}{\zeta_{i+p+1}-\zeta_{i+1}}N_{i+1,p-1}(\zeta) \tag{5}$$

All the derivatives of $N_{i,p}(\zeta)$ exist in the interior of a knot span. An important property is that:

- At a knot, $N_{i,p}(\zeta)$ is $p-l$ times continuously differentiable if the knot has multiplicity l.

Hence increasing knot multiplicity decreases continuity. In other words, the knot vector may contain repeated values depending on the type of continuity that is intended to be assigned to the geometry representation obtained by the B-splines. For instance, a double repeated knot for degree $p=2$ implies a corner of the boundary (i.e. C^0 continuity). Infact:

- In the knots with multiplicity p, $N_{i,p}$ is C^0, its value in that knot is 1 and its control point is coincident with the knot.

A generic curve representing the boundary of an elastic domain subjected to generic static loads can be represented by the aid of the NURBS, that is:

$$\mathbf{x}(\zeta) = \sum_{k=1}^{n} R_{k,p}(\zeta)\mathbf{P}^{\textcircled{k}} \tag{6}$$

where $\mathbf{P}^{\textcircled{k}}$ is the k^{th} control point. The curve is closed if first and last control points are coincident.

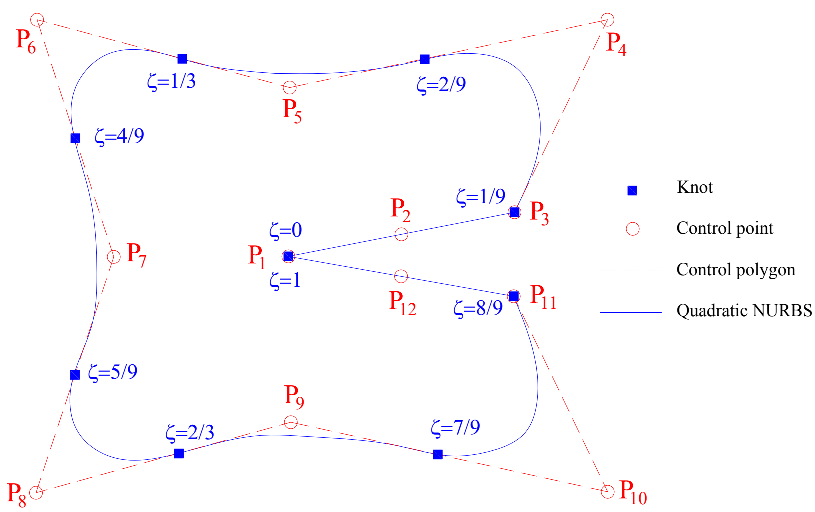

Figure 1: Example of boundary represented by NURBS: geometry.

An example of boundary representation by quadratic ($p = 2$) NURBS is given in Fig. 1, where the control points are depicted by red circles and the knots by blue squares. The normalized knot vector is given by:

$$U = (0,0,0,\frac{1}{9},\frac{1}{9},\frac{2}{9},\frac{1}{3},\frac{4}{9},\frac{5}{9},\frac{2}{3},\frac{7}{9},\frac{8}{9},\frac{8}{9},1,1,1) \tag{7}$$

The corresponding shape functions NURBS are drawn in Fig. 2 where the curves from left to right are $N_{1,2},\cdots,N_{13,2}$ (13 is the number of the control points with the first counted twice as it is coincident with the last one).

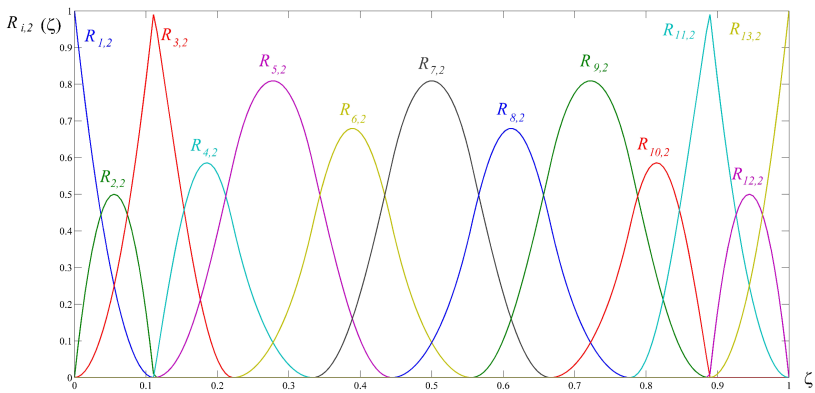

Figure 2: NURBS associated to the example in Fig. 1.

From the figure it is evident that the third NURBS assumes the unit value in the knot as that knot, $\zeta_i = \frac{1}{9}$, is repeated twice.

3 BEM and the IGABEM

The governing integral equation in linear elasticity is given by:

$$c_{ij}(\xi)u_j(\xi) + \int_\Gamma T^*_{ij}(\xi,\mathbf{x})u_j(\mathbf{x})d\Gamma(\mathbf{x}) \quad = \quad \int_\Gamma U^*_{ij}(\xi,\mathbf{x})t_j(\mathbf{x})d\Gamma(\mathbf{x}) \tag{8}$$

where $c_{ij}(\xi)$ is the well-known free term computed in ξ, $T^*_{ij}(\xi,\mathbf{x})$, $U^*_{ij}(\xi,\mathbf{x})$ are the classical Kelvin fundamental solution, i.e. displacements and tractions in $\mathbf{x}$, respectively, in the i direction for a unit load acting along the j direction in a point ξ of the infinite elastic plane, ξ and $\mathbf{x}$ represent the source point and the integration point respectively. The expressions of the fundamental solutions T^*_{ij} and U^*_{ij} can be found in Wrobel and Aliabadi (1996) in terms of the radius r, i.e. the distance between the source point and the integration point.

The boundary is then discretized in EL elements characterised by $p+1$ shape functions $M^n(\zeta)$ and jacobian $J^l(\zeta)$, being ζ the local dimensionless variable. By collocating the discretized integral equation in p x EL collocation nodes and after including well-posed boundary conditions, it is possible to obtain a final squared system of equations that can be generally written as:

$$A\mathbf{x} = \mathbf{b} \tag{9}$$

where $\mathbf{x}$ collects the unknowns. Such a system of equations can be solved by any direct or iterative procedure in order to provide the vector of unknowns $\mathbf{x}$.

After solving the matrix Eq. 9 and computing the unknown vector $\mathbf{x}$, it is possible to determine the stress in any interior point by the following integral equation:

$$\sigma_{ij}(\mathbf{X}) \quad = \quad \int_\Gamma U^*_{ijk}(\mathbf{X},\mathbf{x})t_k(\mathbf{x})d\Gamma(\mathbf{x}) - \int_\Gamma T^*_{ijk}(\mathbf{X},\mathbf{x})u_k(\mathbf{x})d\Gamma(\mathbf{x}) \tag{10}$$

The fundamental solutions $T^*_{ijk}(\xi,\mathbf{x})$ and $U^*_{ijk}(\xi,\mathbf{x})$ are related to the fundamental solutions T^*_{ij} and U^*_{ij} by differentiation and application of the Hooke's law. Their expression is provided, among others, in Wrobel and Aliabadi (1996).

The expression of the discretized integral equations, the strategy to compute the singular integrals and the imposition of the boundary conditions are different between the conventional BEM and the IGABEM. In the subsequent subsections such differences will be highlighted.

3.1 Conventional BEM

In the conventional BEM, geometry and physical variables are described by polynomial shape functions. In 2D such functions are the same that are adopted in the FE context with reference to one dimensional problems. In principle any variability is allowed. Constant (actually superparametric as with linear geometry), are for instance often adopted in acoustics. Linear and quadratic isoparametric elements are common choices in elasticity:

$$\begin{array}{cc} \text{Linear shape functions} & \text{Quadratic shape functions} \\ M_1(\zeta) = \frac{1}{2}(1-\zeta) & M_1(\zeta) = \frac{1}{2}\zeta(\zeta-1) \\ M_2(\zeta) = \frac{1}{2}(1+\zeta) & M_2(\zeta) = (1-\zeta)(1+\zeta) \\ & M_3(\zeta) = \frac{1}{2}\zeta(\zeta+1) \end{array} \tag{11}$$

The polynomial shape functions are expressed in terms of the local variable $\zeta \in [-1,1]$, hence allowing a straight application of the common quadrature schemes, and they assume the unit value in one node and zero in the others.

In conventional BEM, therefore, the geometry is described by the following relations :

$$\mathbf{x}(\zeta) = \sum_{k=1}^{p+1} M_k(\zeta)\mathbf{x}^{(k)} \tag{12}$$

and the physical space as follows:

$$\mathbf{u}(\zeta) = \sum_{k=1}^{p+1} M_k(\zeta)\mathbf{u}^{(k)} \tag{13a}$$

$$\mathbf{t}(\zeta) = \sum_{k=1}^{p+1} M_k(\zeta)\mathbf{t}^{(k)} \tag{13b}$$

where p is the order of the shape function ($p = 1$ for linear elements and $p = 2$ for quadratic elements, for instance), $\mathbf{x}^{(k)}$ are the coordinates of the k^{th} node of the element, $\mathbf{u}^{(k)}$ and $\mathbf{t}^{(k)}$ displacement and traction in the k^{th} node of the element. The discretization of the boundary performed with the above element leads to the following boundary integral equation:

$$\begin{aligned} &c_{ij}(\boldsymbol{\xi})u_j(\boldsymbol{\xi}) + \sum_{l=1}^{EL}\sum_{k=1}^{p+1} u_j^{(k)} \int_{-1}^{+1} T^*_{ij}(\boldsymbol{\xi},\mathbf{x}(\zeta))M_k(\zeta)J_l(\zeta)d\zeta \\ &= \sum_{l=1}^{EL}\sum_{k=1}^{p+1} t_j^{(k)} \int_{-1}^{+1} U^*_{ij}(\boldsymbol{\xi},\mathbf{x}(\zeta))M_k(\zeta)J_l(\zeta)d\zeta \end{aligned} \tag{14}$$

where $J_l(\zeta)$ is the Jacobian of the transformation (Eq. 12). The above equation can be collocated in each node (p x EL totally) to obtain:

$$H\mathbf{u} = G\mathbf{t} \tag{15}$$

where **u** and **t** collect the displacement and the traction vectors in each collocation node.

Two singular integrals arise when the integration is carried out on the element containing the collocation node. The integral involving U_{ij} is weakly singular and it does not present special issue for implementation; it can be computed by using a special quadrature formula for the logarithmic part of the fundamental solution. The integral involving T_{ij} is strongly singular and it deserves special attention; in conventional BEM it is usually computed by applying the rigid body condition that allows the evaluation of the diagonal term as sum of the off-diagonal entries.

The system of equations Eq. 15 can be arranged by correctly applying the boundary conditions, i.e. by imposing two scalar conditions (in 2D) in each boundary node in terms of either the displacement component or the traction component. Such boundary conditions can be directly applied to the unknowns (either u_i or t_i) and provide the final square system of equations Eq. 9 with $\mathbf{x}$ collecting the unknown traction/displacement components.

3.2 IGABEM

The geometry of the boundary can be represented by the relation given in Eq. 6 in terms of the control points and of the knot vector. This is the first difference with the conventional BEM: the NURBS allows a more powerful geometrical representation and a simpler link with the CAD softwares. One feature is that the geometry is described in terms of geometrical nodes, the control points, that do not necessarily lie on the boundary.

It is obvious that the NURBS of degree 0 and 1 are coincident with the polynomial shape functions.

The NURBS can also be used for the describing the governing physical variables, i.e. displacement and traction vectors:

$$\mathbf{u}(\zeta) = \sum_{k=1}^{n} R_{k,p}(\zeta)\mathbf{d}^{(k)} \tag{16a}$$

$$\mathbf{t}(\zeta) = \sum_{k=1}^{n} R_{k,p}(\zeta)\mathbf{q}^{(k)} \tag{16b}$$

where the sum is computationally carried out for each point ζ on the non-zero $p+1$ terms out of the n terms, with n being the total number of control points. On the basis of the discretization carried out by Eq. 6 and Eq. 16, the discretized integral equation can be written as:

$$\begin{aligned} c_{ij}(\boldsymbol{\xi}) \sum_{k=1}^{p+1} R_{k,p}(\boldsymbol{\xi}) d_j^{(k)} + \sum_{e=1}^{NE} \sum_{k=1}^{p+1} d_j^{(k)} \left[\int_{\Gamma_e} T_{ij}^*(\boldsymbol{\xi}, \mathbf{x}(\zeta)) R_{k,p}(\zeta) J_l(\zeta) d\zeta \right] \\ = \sum_{e=1}^{NE} \sum_{k=1}^{p+1} q_j^{(k)} \left[\int_{\Gamma_e} U_{ij}^*(\boldsymbol{\xi}, \mathbf{x}(\zeta)) R_{k,p}(\zeta) J_l(\zeta) d\zeta \right] \end{aligned} \tag{17}$$

It must be pointed out that the sum on k should be carried out on n terms but one of the properties listed in the previous Section ensures that in each boundary element at most $p+1$ NURBS are non zero. The element Γ_e must be intended as the part of curve going from ζ_r to ζ_{r+1} of the knot vector, provided that ζ_r is the e^{th} knot without counting the multiplicity and $\zeta_r \neq \zeta_{r+1}$. $J_l(\zeta)$ is the Jacobian of the map given by Eq. 6. The unknowns $\mathbf{d}^{ⓚ}$ and $\mathbf{q}^{ⓚ}$ do not represent, as it occurs in conventional BEM, the values of displacement and traction, respectively, in the node, but they are variables that have neither physical meaning nor relation with $\mathbf{u}$ and $\mathbf{t}$. Only one observation can be taken: after $\mathbf{d}$ is computed, the deformed geometry can be drawn by using new control points that are shifted from the initial position of the quantity $\mathbf{d}$.

Different strategies are available to set the position of the collocation points $\overline{\zeta}$. The one adopted in the present paper is given by the Greville abscissae, i.e:

$$\overline{\zeta}_i = \frac{\zeta_{i+1} + \cdots + \zeta_{i+p}}{p} \tag{18}$$

where ζ_i is the i^{th} knot.

Fig. 3 provides an example of subdivision of elements and location of collocation points as given by Eq. 18.

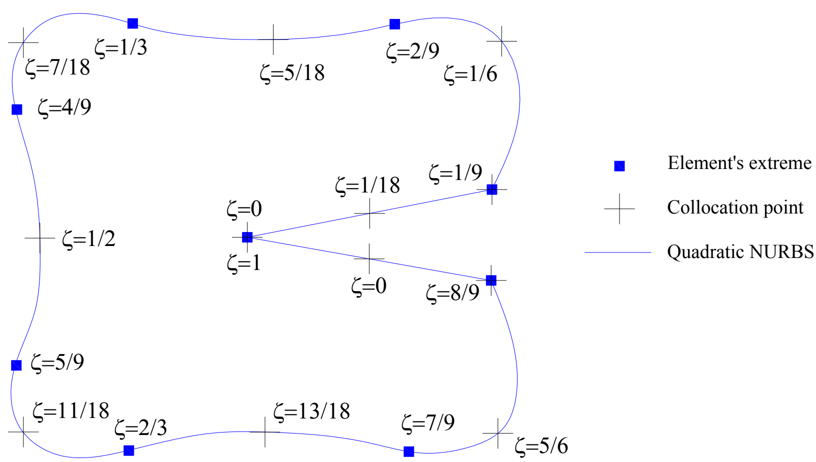

Figure 3: Example of boundary represented by NURBS: element's extremes and collocation nodes

In analogous way can be obtained the discretized expression providing the stress in any interior point.

Collocating Eq. 17 in each collocation point provides the following system of equations:

$$Hd = Gq \tag{19}$$

The non-singular integrals involved in Eq. 17 can be computed by Gaussian quadrature after a variable transformation $\zeta \rightarrow \eta$ that allows $\int_{\Gamma_e}$ to be transformed into $\int_{-1}^{+1}$. If V_{ij} represents either U^*_{ij} or T^*_{ij}, we have:

$$\int_{\Gamma_e} V_{ij}(\boldsymbol{\xi},\mathbf{x}(\zeta))R_{k,p}(\zeta)J_l(\zeta)d\zeta = \int_{-1}^{+1} V_{ij}(\boldsymbol{\xi}(\eta),\mathbf{x}(\zeta(\eta)))R_{k,p}(\zeta(\eta))J_l(\zeta(\eta))J_l^{\eta}d\eta \tag{20}$$

where the Jacobian J_l^{η} is constant and it can be easily computed (see for instance Appendix C in Simpson, Bordas, Trevelyan, and Rabczuk (2012)).

The integral involved in U^*_{ij} for $\overline{\zeta}_i \in \Gamma_e$ is weakly singular and it can be carried out by performing the transformation technique proposed by Telles (1987). On the other hand, in the same situation, the T^*_{ij} integral is strongly singular: the well-known rigid body condition cannot be applied as the NURBS are not guaranteed to assume the unit value in each collocation node (see also par. 4.4.1 in Simpson, Bordas, Trevelyan, and Rabczuk (2012) for a more detailed explanation). For this reason the direct computation is necessary. The singularity-subtraction technique proposed by Guiggiani and Casalini (1987) is here adopted.

4 Imposition of the boundary conditions in IGABEM

It is not straightforward to apply the boundary conditions to the matrix system represented by Eq. 19. The unknowns are parameters that have no physical meaning whereas the boundary conditions are to be applied directly to the collocation nodes in terms of either displacement or traction. To apply inhomogeneous boundary conditions may introduce an error that reduces the overall accuracy. In the present section a new procedure is provided to overcome such a issue.

Let us consider general mixed well-posed boundary conditions. For the sake of simplicity we suppose that the discrete boundary conditions are imposed to the collocation points. The proposed procedure is general and it can be easily adapted in case different locations are set. On the basis of the Eq. 16 it is possible to state the boundary conditions as follows:

$$\overline{\mathbf{w}} = B\mathbf{v} = \begin{bmatrix} B_d & B_q \end{bmatrix} \begin{pmatrix} \mathbf{d} \\ \mathbf{q} \end{pmatrix} \tag{21}$$

The vector $\overline{\mathbf{w}}$ collects the $2n$ values, displacement or traction component, imposed on the n boundary collocation nodes, i.e.:

$$\overline{\mathbf{w}} = [\overline{u}_{1or2}(\zeta_1)\ or\ \overline{t}_{1or2}(\zeta_1), \cdots\cdots, \overline{u}_{2or1}(\zeta_n)\ or\ \overline{t}_{2or1}(\zeta_n)]^T \tag{22}$$

with T meaning transpose. Let us remind that n is the number of control points, and that it is coincident with the total number of the involved NURBS shape functions as well as with the total number of collocation points.

The matrix B is a ($2n$ x $4n$) matrix that can be decomposed into two squared submatrices, B_d and B_q, of equal size ($2n$ x $2n$). For general mixed boundary conditions, the non-zero rows of the submatrix B_d have exactly the same entries of the non-zero rows of the submatrix B_q, the only difference being the different location of the row. This implies that only the entries of one of them need to be computed. In the particular cases of Dirichlet and Neumann boundary conditions, we have $B_q = 0$ and $B_d = 0$, respectively. If the i^{th} row of B_d has non-zero entries, its $(i, j)^{th}$ element is the value of $R_{j,p}$ computed in the collocation node ζ_I where $I = i/2 + r(i/2)$ and $r(i/2)$ is the remainder of the integer division $i/2$.

The columns of the matrix B can be arranged in order to have all the unknowns in $\mathbf{x}$ and all the variables involved by the boundary conditions in $\mathbf{y}$, i.e.:

$$\overline{\mathbf{w}} = \begin{bmatrix} B_x & B_y \end{bmatrix} \begin{pmatrix} \mathbf{x} \\ \mathbf{y} \end{pmatrix} \tag{23}$$

If for instance the boundary conditions in the collocation node ζ_3 are $u_1 = \overline{u}_1$ and $t_2 = \overline{t}_2$, then q_1, d_2 are included in $\mathbf{x}$ whereas d_1, q_2 are shifted in $\mathbf{y}$.

A matrix condensation is now possible, i.e.:

$$\mathbf{y} = -B_y^{-1} B_x \mathbf{x} + B_y^{-1} \overline{\mathbf{w}} = C\mathbf{x} + \mathbf{a} \tag{24}$$

The system of equations Eq. 19 previously introduced can be updated to obtain the final system to be solved. In fact, by a simple rearrenging of the columns of H and G we have:

$$H\mathbf{d} = G\mathbf{q} \Longrightarrow A\mathbf{x} = L\mathbf{y} \tag{25}$$

Finally, the vector $\mathbf{y}$ can be replaced by Eq. 24 to give:

$$(A - LC)\mathbf{x} = L\mathbf{a} \Longrightarrow \overline{A}\mathbf{x} = \mathbf{b} \tag{26}$$

that is the final system of equations in which the boundary conditions have been imposed correctly to the boundary points.

5 Numerical results

The numerical integration within each non-singular element is carried out by twelve-points Gauss quadrature rule. Sixteen Gaussian points are used in the vicinity of the boundary in order to deal with near-singularity problems in the computations of the internal stress. The boundary stress is computed by expressing the traction in a local coordinate system and employing the relationship between strain displacements on the tangent direction to the boundary with the aid of the shape functions Telles and Brebbia (1979). In the legends accompanying the graphs the term "IGABEM" is associated to the numerical results in which the boundary conditions are directly applied to the control variables, whereas "IGABEM-impr" denotes the application of the (improved) present approach.

All the error norms are normalized with respect to their corresponding norms computed from the analytical solution, i.e.:

$$e = \frac{||\mathbf{u} - \mathbf{u}_{an}||_{L_2}}{||\mathbf{u}_{an}||_{L_2}} \tag{27}$$

A numerical example, for which an analytical solution is available, is presented to demonstrate the efficiency of the proposed procedure: an hollow cylinder is loaded internally and externally. The geometry parameters are: outer radius $r_e = 1.0$, inner radius $r_i = 0.2$ (see Fig. 4). The mechanical parameters are: Young's modulus $E = 100000$ and Poisson's coefficient $\nu = 0.3$. The prescribed boundary conditions are: external pressure $p_e = 2$ and internal pressure $p_i = 1$. In such a case an analytical solution is available (see for instance Eqs. 24-25 in Mallardo and Alessandri (2000)) and thus compared to the numerical one. Geometry and loads of the example, along with the index space, parametric space, control net and the physical mesh, are depicted in Fig. 4. Each of the two circles is initially generated as four NURBS: it is worthy to underline that four NURBS are able to describe the geometry of the circle exactly.

The results are listed in Tab. 1, where a comparison between analytical, IGABEM and IGABEM-impr numerical values is carried out with reference to the points A and B depicted in Fig. 4. The numerical results are obtained by meshing four elements on the external circle and four elements on the internal one. The error in the second and in the fourth column is computed as:

$$\text{err} = \frac{|u_r^{an} - u_r^{num}|}{|u_r^{an}|} \tag{28}$$

It is worthy to underline that a classical BEM approach would require minimum 12 quadratic elements for each circle in order to obtain the same accuracy.

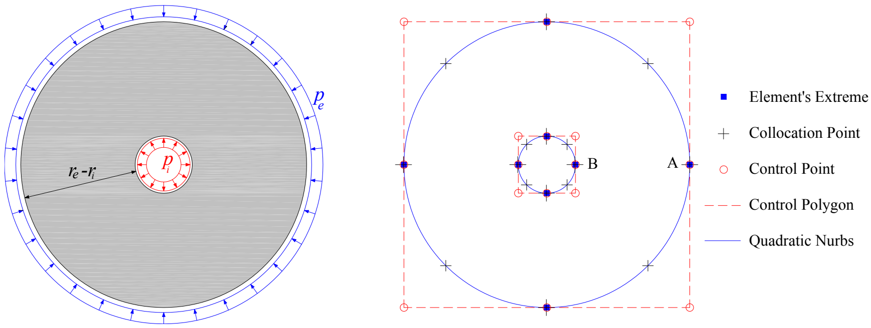

Figure 4: Description of the hollow cylinder example with related NURBS and boundary discretization

Table 1: Comparison of the radial displacement.

	$\lvert u_r(A)\rvert \cdot 10^4$	err(%)	$\lvert u_r(B)\rvert \cdot 10^4$	err (%)
analytic	0.111583	-	0.048317	-
IGABEM	0.106702	4.38	0.042299	12.45
IGABEM-impr	0.111581	$2.3 \cdot 10^{-3}$	0.048318	$3.2 \cdot 10^{-3}$

Three different meshes are used in order to test the convergence performance. The series of used meshes is depicted in Fig. 5.

The convergence comparison is depicted in Fig. 6 where the superior solution accuracy with the desired rates of convergence is easily observed. In the figure h measures the average length of the element

6 Conclusions

An improved IGABEM approach has been presented. In the common approach the boundary conditions are directly applied to the control variables: the function describing the boundary condition is evaluated at the spatial locations of the control points and then the resultant values are assigned to the corresponding control variables. Such an approach may introduce an error that jeopardizes the final accuracy. In this work an improved IGABEM approach has been presented with enhanced treatment of the boundary conditions. The procedure stems from a suitable transformation relationship that allows a straightforward imposition of the boundary conditions and, hence, a simple reassembling of the governing final system of equations. The effectiveness of the method has been validated by one elasticity problem. Numerical results have shown that the present approach produces a

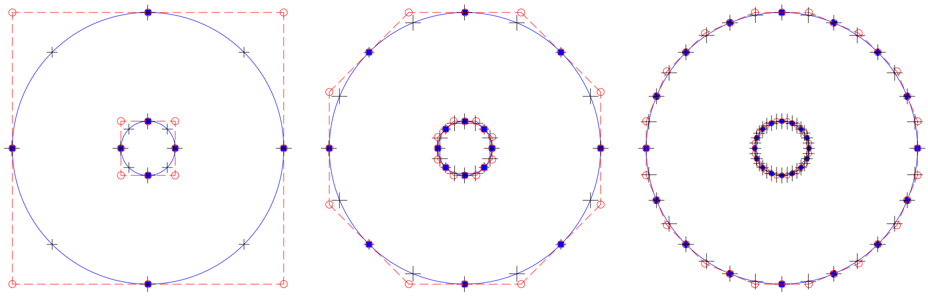

Figure 5: Three meshes adopted in the hollow cylinder example. The legend is the same of Fig. 4.

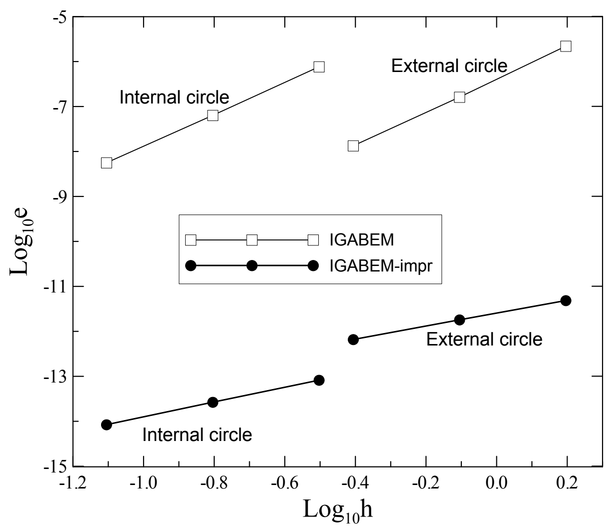

Figure 6: Comparison of the L_2-error norm for the hollow cylinder example.

higher accuracy and better convergence rates compared with the classical IGABEM formulation involving direct enforcement of the boundary conditions to the control variables. The higher the distance between the control points and the boundary, the better the performance of the proposed approach.

References

Cho, M.; Choi, J.; Roh, H. (2008): Integration of shell FEA with geometric modeling on Nurbs surface representation for practical applications. *CMES: Computer Modeling in Engineering & Sciences*, vol. 33, pp. 17–47.

Costantini, P.; Manni, C.; Pelosi, F.; Sampoli, M. L. (2010): Quasi-interpolation in isogeometric analysis based on generalized B-splines. *Computer Aided Geometric Design*, vol. 27, pp. 656–668.

Guiggiani, M.; Casalini, P. (1987): Direct computation of cauchy principal value integrals in advanced boundary elements. *International Journal for Numerical Methods in Engineering*, vol. 24, pp. 1711–1720.

Hughes, T.; Cottrell, J.; Bazilev, Y. (2005): Isogeometric analysis: CAD, finite elements, NURBS, exact geometry and mesh refinement. *Computer Methods in Applied Mechanics and Engineering.*, vol. 194, pp. 4135–4195.

Mallardo, V. (2009): Integral equations and nonlocal damage theory: a numerical implementation using the BDEM. *International Journal of Fracture*, vol. 157, pp. 13–32.

Mallardo, V.; Alessandri, C. (2000): Inverse problems in the presence of inclusions and unilateral constraints: a boundary element approach. *Computational Mechanics*, vol. 26, pp. 571–581.

Mallardo, V.; Aliabadi, M. (2012): An adaptive Fast Multipole approach to 2D wave scattering. *CMES: Computer Modeling in Engineering & Sciences*, vol. 87, pp. 77–96.

Peake, M.; Trevelyan, J.; Coates, G. (2013): Extended isogeometric boundary element method (XIBEM) for two-dimensional Helmholtz problems. *Computer Methods in Applied Mechanics and Engineering*, vol. 259, pp. 93–102.

Piegl, L.; Tiller, W. (1997): *The NURBS book.* Springer.

Sageresan, N.; Drathi, R. (2008): Crack propagation in concrete using meshless method. *CMES: Computer Modeling in Engineering & Sciences*, vol. 32, pp. 103–112.

Sevilla, R.; Fernández-Méndez, S.; Huerta, A. (2008): NURBS-enhanced finite element method (NEFEM). *International Journal for Numerical Methods in Engineering*, vol. 76, pp. 56–83.

Sevilla, R.; Fernández-Méndez, S.; Huerta, A. (2011): 3D NURBS-enhanced finite element method (NEFEM). *International Journal for Numerical Methods in Engineering*, vol. 88, pp. 103–125.

Shaw, A.; Banerjee, B.; Roy, D. (2008): A NURBS-based parametric method bridging mesh-free and finite element formulation. *CMES: Computer Modeling in Engineering & Sciences*, vol. 26, pp. 31–57.

Shaw, A.; Roy, D. (2008): NURBS-based parametric mesh-free methods. *Computer Methods in Applied Mechanics and Engineering*, vol. 197, pp. 1013–1034.

Simpson, R.; Bordas, S.; Lian, H.; Trevelyan, J. (2013): An isogeometric boundary element method for elastostatic analysis: 2D implementation aspects. *Computers and Structures*, vol. 118, pp. 2–12.

Simpson, R.; Bordas, S.; Trevelyan, J.; Rabczuk, T. (2012): A two-dimensional Isogeometric Boundary Element Method for elastostatic analysis . *Computer Methods in Applied Mechanics and Engineering*, vol. 209-212, pp. 87–100.

Sunilkumar, N.; Roy, D. (2010): A smooth Finite Element Method based on reproducing Kernel DMS-Splines. *CMES: Computer Modeling in Engineering & Sciences*, vol. 65, pp. 107–153.

Takahashi, T.; Matsumoto, T. (2012): An application of fast multipole method to isogeometric boundary element method for Laplace equation in two dimensions. *Engineering Analysis with Boundary Elements*, vol. 36, pp. 1766–1775.

Telles, J. (1987): A self-adaptive co-ordinate transformation for efficient numerical evaluation of general boundary element integrals. *International Journal for Numerical Methods in Engineering*, vol. 24, pp. 959–973.

Telles, J.; Brebbia, C. (1979): On the application of the boundary element method to plasticity. *Applied Mathematical Modelling*, vol. 3, pp. 466–470.

Wang, D.; Xuan, J. (2010): An improved NURBS-based isogeometric analysis with enhanced treatment of essential boundary conditions. *Computer Methods in Applied Mechanics and Engineering*, vol. 199, pp. 2425–2436.

Wrobel, L.; Aliabadi, M. (1996): *The Boundary Element Method, Vol. 2: Applications in Solids and Structures*. Wiley.